SUPPLEMENTARY MATERIAL

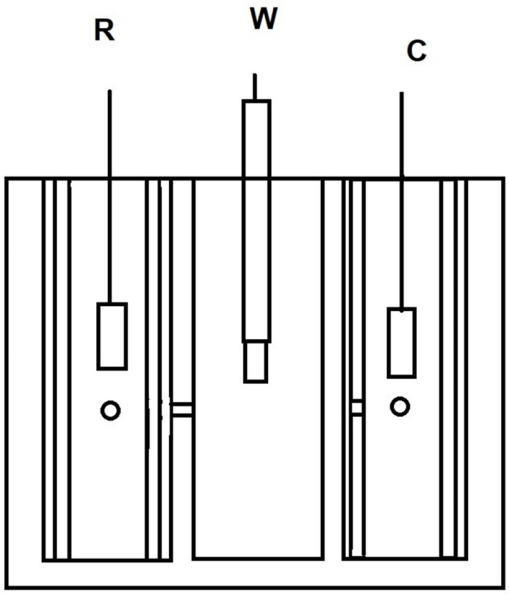


Figure S1. Scheme of the PFTE cell used in the electrochemical measurements. R: reference electrode, W: working electrode, C: counter electrode

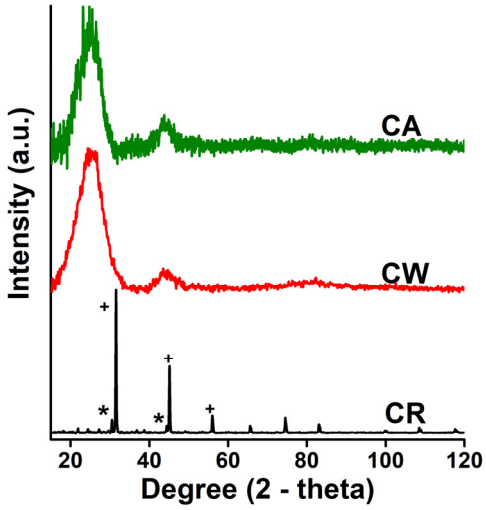


Figure S2. XRD diffractograms of the carbon aerogel samples. Peaks labeled with + and * correspond to calcium sulfide (CaS) and potassium sodium sulfate ($KNaSO_4$), respectively.

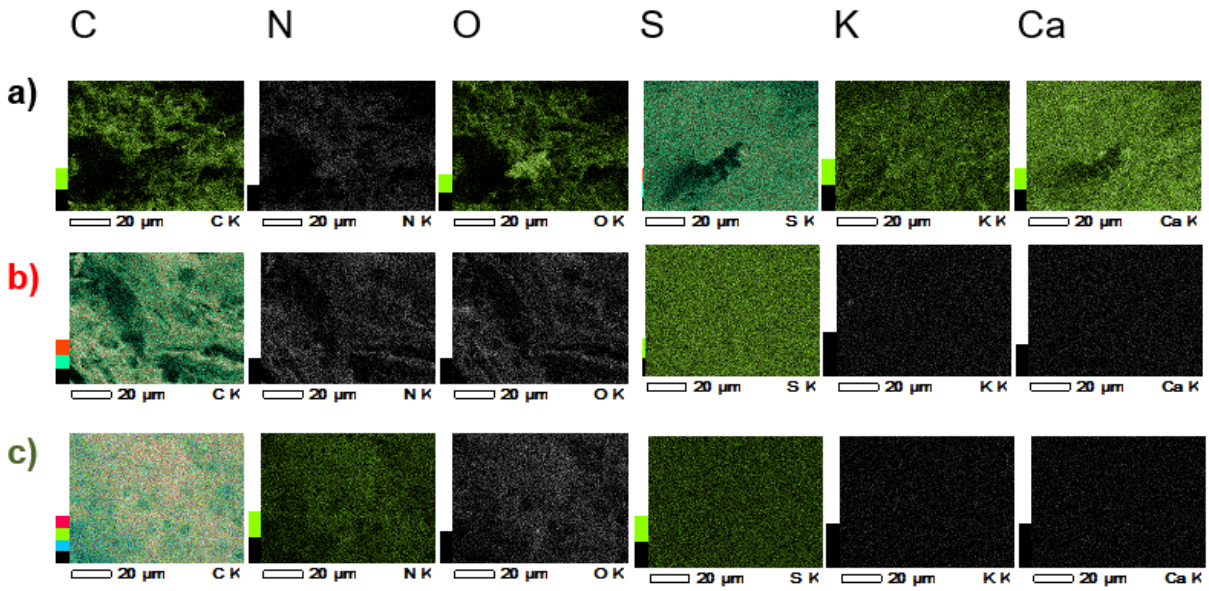


Figure S3. Elemental mapping from SEM-EDS analysis. (**a**) CR; (**b**) CW; (**c**) CA.

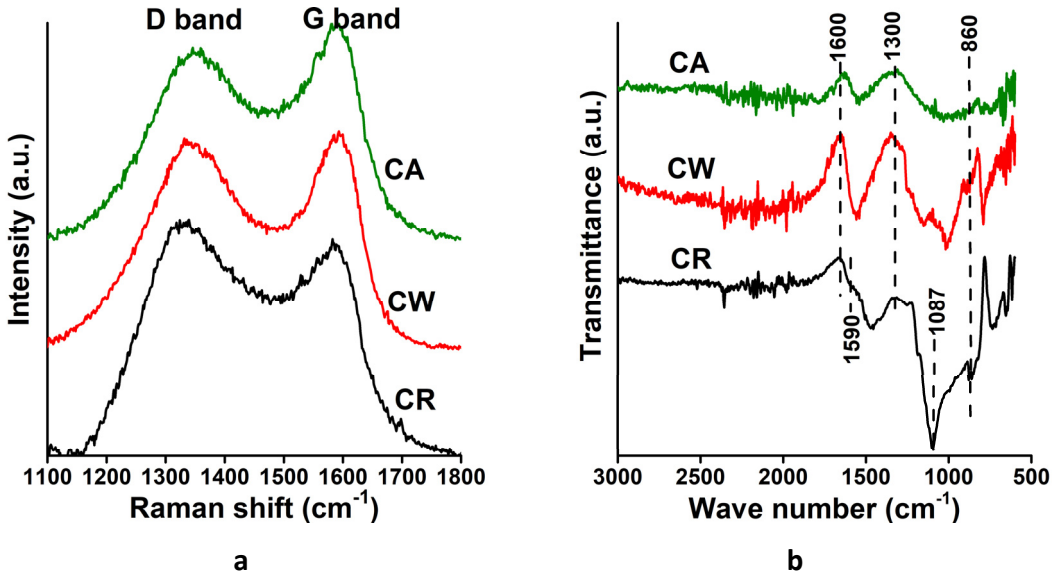


Figure S4. (**a**) Baseline corrected and normalized Raman spectra. ID/IG ratios are 1.06, 0.94, 0.95 for the CR, CW, and CA samples, respectively. (**b**) FTIR spectra of the precursors and CA. The range from 860 to 1300 cm^{-1} corresponds to the C-O stretching vibrations [69–71], and the signal reduces significantly after washing and annealing steps because of the decrease in the oxygen content. A clear peak at 1087 cm^{-1} appears in the spectrum for carbon raw (CR) and corresponds to S=O stretching [71]; this agrees with the presence of sulfur in the raw carbon, which is removed later with the acid washing. Also, the spectrum for the CR sample shows a small signal around 1590 cm^{-1} which corresponds to N-H bending vibration [71], but it is not distinguishable in the two other samples. The signal at 1300–1600 cm^{-1} corresponds to C=C from unoxidized sp^2 C-C bonds [69], O-H bending, C-OH stretching [70], and C-H bending vibrations [71]. This signal increases in the washed sample due to the acid washing step, but it becomes smaller in the annealed sample.

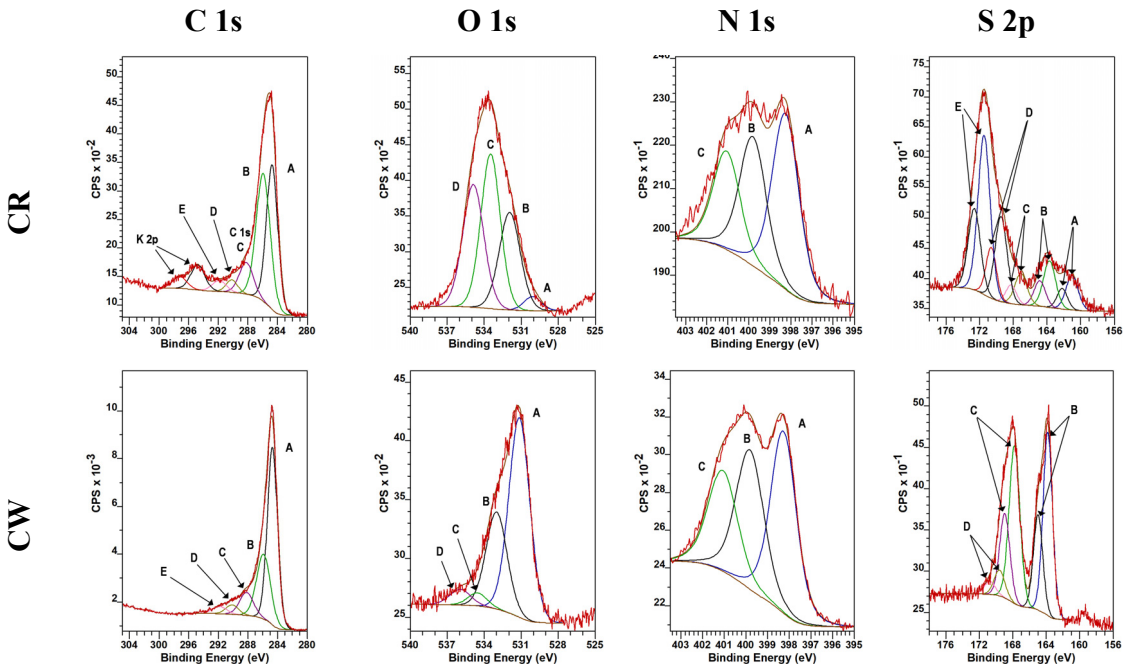


Figure S5. Deconvoluted regions of the XPS spectra of the porous carbon intermediates.

Table S1. Elemental compositions (atomic %) measured by EDS.

Sample	C	O	N	S	K	Ca	Na
CR	44.3	23.6	8.6	9.2	3.9	9.1	1.2
CW	73.4	6.3	17.5	2.8	n.d. *	n.d. *	n.d. *
CA	73.3	4.1	21.7	0.8	n.d. *	n.d. *	n.d. *

* n.d.: not detected

Table S2. Assignation of the chemical states in the C1s, O1s, N1s, and S2p 3/2 regions.

Measured Energy (eV)	Label in Figures	Assignation	Component Ratios			Ref
			CR	CW	CA	
C 1s						
284.66–284.73	A	graphitic C, disordered sp2 C-C	39.6	55.5	59.5	[18]
285.86–285.93	B	C-OH, epoxide	42.8	27.8	23.7	
288.16–288.23	C	C=O carbonyl	10.6	9.8	9.1	
290.11–290.18	D	O=C-OH carbonate	3.4	3.7	4.1	
291.81–291.88	E	π-π* shake up	3.7	3.2	3.6	
O 1s						
530.08–530.16	A	O=C-OH, adsorbed O	3.1	61.6	12.4	[18]
531.93–532.01	B	quinine	26.1	30.0	56.2	
533.48–533.56	C	C-O-C, O=C-O*	38.1	3.6	29.4	
534.88–534.96	D	O related to S/N?	32.8	4.8	2.1	
N 1s						
398.25	A	N-N pyridinic	43.6	40.6	46.0	[18]
399.80	B	pyrrolic N	32.0	33.8	5.9	
400.95–401.06	C	quaternary N, sp2 N in rings	46.0	5.9	48.1	
S 2p						
161.01	A	thiol (-SH)	9.6	n.d.	n.d.	[72]
163.69–163.88	B	2p3/2 (S1) and 2p1/2 (S2) positions of thiophene-S	13.1	46.8	100	[73,74]
167.09–167.79	C	-C-SO2-	8.8	45.7	n.d.	[74]
169.46–169.58	D	-C-SO4-	23.8	7.5	n.d.	
171.47	E	RO2-S-S-R, R-SO3H (in sulfonic acids)	44.6	n.d.	n.d.	[13]

References in supplementary material

69 Marcano, C. D.; Kosynkin, D. V.; Berlin, J. M.; Sinitskii, A.; Sun, Z.; Slesarev, A.; Alemany, L. B.; Lu, W.; Tour, J. M. Improved synthesis of graphene oxide. *ACS Nano* **2010**, *4*, 4806–4814.

70 Fernández-Merino, M. J.; Guardia, L.; Paredes, J. I.; Villar-Rodil, S.; Solís-Fernández, P.; Martínez-Alonso, A.; Tascón, J. M. D. RVitamin C is an ideal substitute for hydrazine in the reduction of graphene oxide suspensions. *J. Phys. Chem. C* **2010**, *114*, 6426–6432.

71. IR Spectrum Table & Chart. Available online: https://www.sigmaaldrich.com/technical-documents/articles/biology/ir-spectrum-table.html (accessed on 6 May 2021).

72. Su, Y.; Zhang, Y.; Zhuang, X.; Li, S.; Wu, D.; Zhang, F.; Feng, X. Low-temperature synthesis of nitrogen/sulfur co-doped three-dimensional graphene frameworks as efficient metal-free electrocatalyst for oxygen reduction reaction. *Carbon* **2013**, *62*, 296–301.
73. Seredych, M.; Khine, M.; Bandosz, T. Enhancement in Dibenzothiophene reactive adsorption from liquid fuel via incorporation of sulfur heteroatoms into the nanoporous carbon matrix. *ChemSusChem* **2011**, *4*, 139–147.
74. Yang, S.; Zhi, L.; Tang, K.; Feng, X.; Maier, J.; Mullen, K. Efficient synthesis of heteroatom (N or S)-doped graphene based on ultrathin graphene oxide-porous silica sheets for oxygen reduction reactions. *Adv. Funct. Mater.* **2012**, *22*, 3634–3640.